

Accuracy of three-dimensional periodontal ligament models generated using cone-beam computed tomography at different resolutions for the assessment of periodontal bone loss

Hangmiao Lyu^a 
Li Xu^b
Huimin Ma^a
Jianxia Hou^b
Xiaoxia Wang^c
Yong Wang^d
Yijiao Zhao^d
Weiran Li^a 
Xiaotong Li^a 

^aDepartment of Orthodontics, National Engineering Laboratory for Digital and Material Technology of Stomatology; Beijing Key Laboratory of Digital Stomatology, Peking University School and Hospital of Stomatology, Beijing, China

^bDepartment of Periodontology, National Engineering Laboratory for Digital and Material Technology of Stomatology; Beijing Key Laboratory of Digital Stomatology, Peking University School and Hospital of Stomatology, Beijing, China

^cDepartment of Oral and Maxillofacial Surgery, National Engineering Laboratory for Digital and Material Technology of Stomatology; Beijing Key Laboratory of Digital Stomatology, Peking University School and Hospital of Stomatology, Beijing, China

^dCenter of Digital Dentistry, Peking University School and Hospital of Stomatology; National Engineering Laboratory for Digital and Material Technology of Stomatology; Research Center of Engineering and Technology for Digital Dentistry of Ministry of Health; Beijing Key Laboratory of Digital Stomatology, Peking University School and Hospital of Stomatology, Beijing, China

Objective: To develop a method for generating three-dimensional (3D) digital models of the periodontal ligament (PDL) using 3D cone-beam computed tomography (CBCT) reconstruction and to evaluate the accuracy and agreement of the 3D PDL models in the measurement of periodontal bone loss. **Methods:** CBCT data collected from four patients with skeletal Class III malocclusion prior to periodontal surgery were reconstructed at three voxel sizes (0.2 mm, 0.25 mm, and 0.3 mm), and 3D tooth and alveolar bone models were generated to obtain digital PDL models for the maxillary and mandibular anterior teeth. Linear measurements of the alveolar bone crest obtained during periodontal surgery were compared with the digital measurements for assessment of the accuracy of the digital models. The agreement and reliability of the digital PDL models were analyzed using intra- and interexaminer correlation coefficients and Bland-Altman plots. **Results:** Digital models of the maxillary and mandibular anterior teeth, PDL, and alveolar bone of the four patients were successfully established. Relative to the intraoperative measurements, linear measurements obtained from the 3D digital models were accurate, and there were no significant differences among different voxel sizes at different sites. High diagnostic coincidence rates were found for the maxillary anterior teeth. The digital models showed high intra- and interexaminer agreement. **Conclusions:** Digital PDL models generated by 3D CBCT reconstruction can provide accurate and useful information regarding the alveolar crest morphology and facilitate reproducible measurements. This could assist clinicians in the evaluation of periodontal prognosis and establishment of an appropriate orthodontic treatment plan.

Key words: Digital models, Three-dimensional reconstruction, Cone-beam computed tomography

Received May 24, 2022; Revised September 20, 2022; Accepted November 16, 2022.

Corresponding author: Weiran Li.

Professor, Department of Orthodontics, National Engineering Laboratory for Digital and Material Technology of Stomatology; Beijing Key Laboratory of Digital Stomatology, Peking University School and Hospital of Stomatology, No. 22 Zhongguancun Nandajie, HaiDian District, Beijing 100081, China.

Tel +86-010-82195381 e-mail weiranli@bjmu.edu.cn

Corresponding author: Xiaotong Li.

Associate Professor, Department of Orthodontics, National Engineering Laboratory for Digital and Material Technology of Stomatology; Beijing Key Laboratory of Digital Stomatology, Peking University School and Hospital of Stomatology, No. 22 Zhongguancun Nandajie, HaiDian District, Beijing 100081, China.

Tel +86-010-82195739 e-mail xiaotonglee@hotmail.com

How to cite this article: Lyu H, Xu L, Ma H, Hou J, Wang X, Wang Y, Zhao Y, Li W, Li X. Accuracy of three-dimensional periodontal ligament models generated using cone-beam computed tomography at different resolutions for the assessment of periodontal bone loss. Korean J Orthod 2023;53(2):77-88. <https://doi.org/10.4041/kjod22.120>

© 2023 The Korean Association of Orthodontists.

This is an Open Access article distributed under the terms of the Creative Commons Attribution Non-Commercial License (<http://creativecommons.org/licenses/by-nc/4.0>) which permits unrestricted non-commercial use, distribution, and reproduction in any medium, provided the original work is properly cited.

INTRODUCTION

The periodontal ligament (PDL) is an aligned fibrous network anchored firmly to the cementum covering the tooth root on one side and the alveolar bone of the jaw on the other side,^{1,2} and it can be represented by the root surface area (RSA) below the alveolar bone crest. The area of contact between tooth roots and the surrounding bone plays an important role in orthodontic and periodontal treatment. It has been proposed that the PDL and alveolar bone are functional units that undergo robust remodeling during orthodontic tooth movement.³ Moreover, the PDL area plays an important role in tooth anchorage,⁴ and morphological changes in the PDL reflect the vertical bone level (VBL).⁵ Quantification of the PDL area can help assess the severity of periodontal disease and the prognosis of orthodontic treatment.

Measurement of the alveolar bone thickness and VBL in the sagittal plane of cone-beam computed tomography (CBCT) images is a well-established method.⁶⁻⁸ Past studies have focused primarily on measurement of the height and thickness of the alveolar bone on the labial and lingual sides of the incisors in the sagittal plane. Evaluation of two-dimensional (2D) measurements without consideration of the three-dimensional (3D) PDL area may not adequately indicate the severity of periodontal lesions. Moreover, 2D linear measurements describe VBL in a one-dimensional manner without taking changes in the root shape into account, thus underestimating the true amount of periodontal loss.⁹⁻¹¹

In other previous studies,^{9,12} microcomputed tomography (micro-CT) data were used to measure the RSA on reconstructed digital models of extracted teeth. However, the micro-CT technique cannot be used for *in situ* examination in human patients because of the unacceptably high radiation exposure.¹³ Unlike micro-CT,^{13,14} CBCT provides data for accurate and reproducible 3D reconstruction of the tooth volume, which is useful in some clinical applications. Moreover, CBCT combined with 3D reconstruction technology has been proven to be an efficient and reliable imaging technique for non-invasive acquisition of data on tooth surfaces *in vivo*.^{14,15} With regard to the assessment of periodontal bone loss, measurements of periodontal defects obtained by CBCT combined with 3D reconstruction have shown very high agreement with measurements obtained during surgery¹⁶ or by micro-CT, regardless of the voxel size.¹⁷

Researchers have also used CBCT to reconstruct the root surface to detect apical root resorption cavities¹⁴ and measure the RSA as an important marker for determination of the periodontal treatment plan and prognosis. However, RSA measurements do not take alveolar bone conditions into account; in recent years, the PDL

surface area, or the RSA below the alveolar bone crest, has been studied as a marker of periodontal health, and researchers have artificially simulated the PDL area using digital models of teeth.^{5,9,10,12,17} Nevertheless, to our knowledge, this is the first study to obtain *in vivo* 3D PDL area measurements in the region of the alveolar bone crest in humans.

In the present study, instead of artificially simulating the alveolar bone crest *in vitro*, we measured the PDL area *in vivo* using 3D CBCT reconstruction. The aims of the study were (1) to utilize the 3D CBCT reconstruction technique to generate 3D virtual models of the teeth, PDL, and alveolar bone; (2) to evaluate the accuracy of the virtual models by comparing digital measurements with direct intraoperative measurements; and (3) to investigate the reproducibility of the method.

MATERIALS AND METHODS

Sample selection

Forty-eight anterior teeth from four patients (two female and two male) with skeletal Class III malocclusion requiring surgical orthodontic treatment and augmented corticotomy (AC) were evaluated in this study at Peking University School and Hospital of Stomatology from May 2021 to October 2021. All patients signed informed consent forms. The study was approved by the Biomedical Ethics Committee of the Peking University School and Hospital of Stomatology (approval number: PKUS-SIRB-201839156) and registered on the Clinical Trials Register as ChiCTR1900021778 (Chinese Clinical Trials Registry Platform of the World Health Organization).

The inclusion criteria were as follows: 1) age > 18 years for male patients and > 16 years for female patients;^{18,19} 2) A point-nasion-B point (ANB) angle of < 0° and overjet of < 0 mm; 3) no more than two sites with a probing depth of ≥ 5 mm in the entire oral cavity, bleeding on probing score of ≤ 20%, and plaque score of ≤ 30%; and 4) labial alveolar bone thickness of < 1 mm around the maxillary and mandibular central incisors, as measured by CBCT. The mean alveolar bone thickness at the root apex of the maxillary and mandibular central incisors was 0.81 ± 0.17 mm and 0.4 ± 0.15 mm, respectively. Patients with poor oral hygiene or uncontrolled periodontal disease were excluded.

All orthodontic treatments were performed by a single orthodontist using a straight-wire fixed appliance (0.022" slot size, MBT prescription). For the maxillary anterior teeth, the arch-wire sequence involved 0.014-, 0.016-, 0.018-, and 0.018 × 0.025-inch nickel-titanium wires before periodontal surgery. For the mandibular anterior teeth, periodontal surgery was performed after bracket bonding without any arch wire in place. Two weeks after periodontal surgery, aligning and leveling

were initiated with 0.014-inch nickel-titanium wires.

Image acquisition

Prior to periodontal surgery, CBCT images were acquired with the NewTom VG device (Aperio Services, Verona, Italy) in the regular scan mode (field of view [FOV], 10 × 10 cm; voltage, 110 kV; current, 3.00 mA; and exposure, 1.8 seconds). The CBCT images were reconstructed using different voxel sizes (0.20, 0.25, and 0.30 mm). To reduce scatter at the occlusal plane, patients were instructed to bite on cotton rolls. Within 24 hours of CBCT image acquisition, the patients underwent intraoral scanning.

Generation of digital models

Digital Imaging and Communication in Medicine (DICOM) files were imported into Mimics 19.0 software (Materialise, Leuven, Belgium). In Mimics, 3D digital models of the anterior teeth and bone *in vivo* were reconstructed. In Mimics, the CBCT images had predefined thresholds that were set to correspond to the tooth or bone density as follows: tooth, 1,200–3,071 segments and bone, 226–3,071 segments. The threshold level was set to most clearly show the tooth anatomy with minimal interference from the surrounding bone and adjacent structures. On each CBCT slice, manual refinement was performed through a 2D slice-by-slice procedure to enhance accuracy by correcting for over- and undercontoured voxels in the tooth volume²⁰ (Figure 1).

The digital models were exported in stereolithographic (STL) format and imported into Geomagic software (Geomagic, Cary, NC, USA). For more realistic digitaliza-

tion of the metal brackets bonded to the teeth, a digital model derived from the intraoral scan was superimposed over the 3D model generated from the CBCT datasets (Figure 2).

Linear measurements of the alveolar bone crest on CBCT-derived digital models

In Geomagic software, the vertical distance between the CEJ and alveolar bone crest parallel to the long axis of the anatomic crown was defined as the VBL. The long axis of the anatomic crown was determined by connecting the lowest point of the labial CEJ curve and the midpoint of the mesial and distal incisal angles. The five selected measurement sites on the digital models were the mesiolabial (VBL_MLa), mesiobacket (VBL_MB), midlabial (VBL_La), distobacket (VBL_DB), and distolabial (VBL_DLa) sites. The La point was chosen at the midlabial site on the surface. Proximal points on the surface, i.e., the MLa and DLa points, were located at the corner of each tooth. The vertical distance between the marginal bone crest and the gingival boundary of the metal bracket was defined as the bone-bracket distance (BBD). The three selected measurement points were the mesiobacket (BBD_MB), midlabial (BBD_La), and distobacket (BBD_DB) points. Detailed information about the measurement procedure is shown in Figure 3. Measurements were made to the nearest 0.01 mm using a linear measurement tool in a quiet and dark room.

Linear measurements of the alveolar bone crest during periodontal surgery

All AC procedures were performed by a single perio-

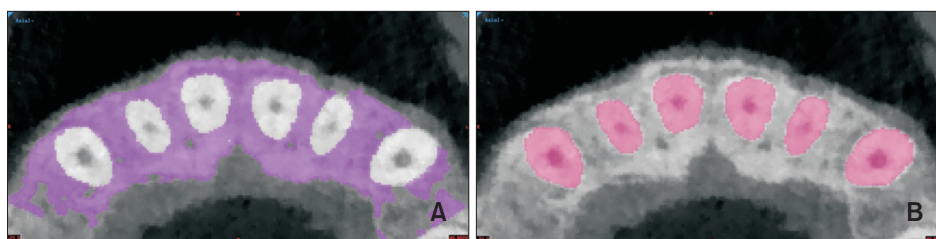


Figure 1. Process of alveolar bone and tooth segmentation in Mimics 19.0 software (Materialise, Leuven, Belgium). **A**, Manual alveolar bone segmentation. **B**, Manual tooth segmentation.

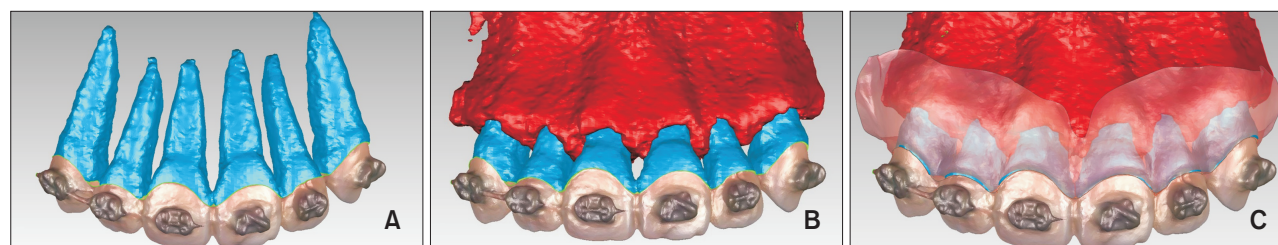


Figure 2. Digital tooth, bone, and soft tissue models in Geomagic (Geomagic, Cary, NC, USA). **A**, Digital tooth models with an intraoral scan superimposed over the crowns. **B**, Digital tooth and bone models. **C**, Digital tooth and bone models generated from cone-beam computed tomography datasets and a soft tissue model derived from an intraoral scan.

dontist using surgical loupes. The AC procedure was performed as follows.²¹ A crevicular incision was made from the canine on one side to the canine on the other side, and a full thickness flap on the labial side was elevated. The distance parallel to the long axis of the anatomic crown between the CEJ and alveolar bone crest was measured at five sites, in addition to the distance between the alveolar bone crest and gingival boundary at the mesial and distal metal bracket sites (Figure 4). All measurements were made to the nearest 1 mm by the same experienced periodontist who performed the AC procedure using a manual periodontal probe (UNC-

15, graded in millimetres; HU-Friedy, Chicago, IL, USA) placed parallel to the long axis of the tooth. The intraoperative measurements were considered the “reference standard.”

Segmentation of the digital PDL

To segment the PDL in the digital model, we identified the alveolar bone crest in the digital model and drew points on the teeth in the model (Figure 5A and 5B). A curve was generated by connecting the points marked on the model surface using the creation method in Geomagic (Figure 5B). The created boundary curve represented the alveolar bone crest (Figure 5C). The teeth were then separated along the curve into two parts (Figure 5D), with preservation of the PDL (Figure 5E), and the PDL area in the digital model was calculated (Figure 5F).

Statistical analysis

Statistical analyses were performed using SPSS 20.0 (IBM Corp., Armonk, NY, USA). All linear measurements for the digital models were obtained twice at an interval of 2 weeks by the same investigator, and the average of these two measurements was used for statistical analysis. The systematic intraexaminer error was determined using a paired *t*-test, and the intraclass correlation coefficient (ICC) was calculated. One-way ANOVA with Duncan’s multiple comparison test was performed to compare linear measurements obtained during surgery and by CBCT at different sites and with different voxel sizes, and the ICC was calculated. Moreover, the Bland–Altman method was applied, and the limits of agreement were identified.

Descriptive statistics for differences between the intraoperative and digital measurements were separately computed. In addition, the 95% confidence interval (CI) was calculated, and diagnostic coincidence rates were calculated using an introduced variable measurement difference to evaluate the accuracy of site-based image

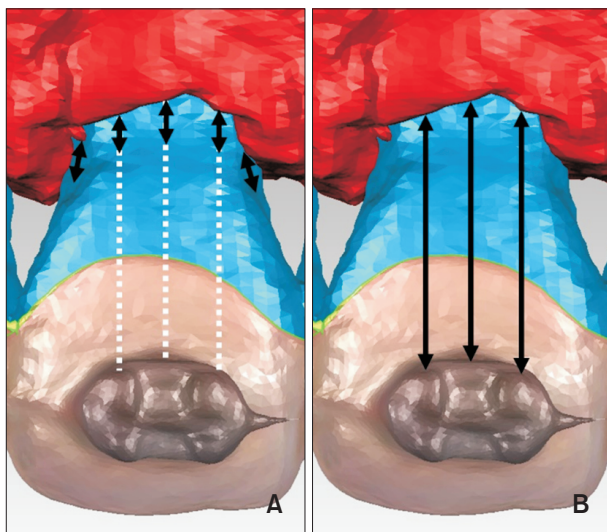


Figure 3. Digital linear measurements. The measurement reference lines at midlabial, distobacket, and distolabial sites are shown (white dotted line). **A**, Vertical bone level measurements (black arrow line) at mesiolabial, mesio-bracket, midlabial, distobacket, and distolabial sites. **B**, Bone–bracket distance measurements (black arrow line) at mesio-bracket, midlabial, and distobacket sites.

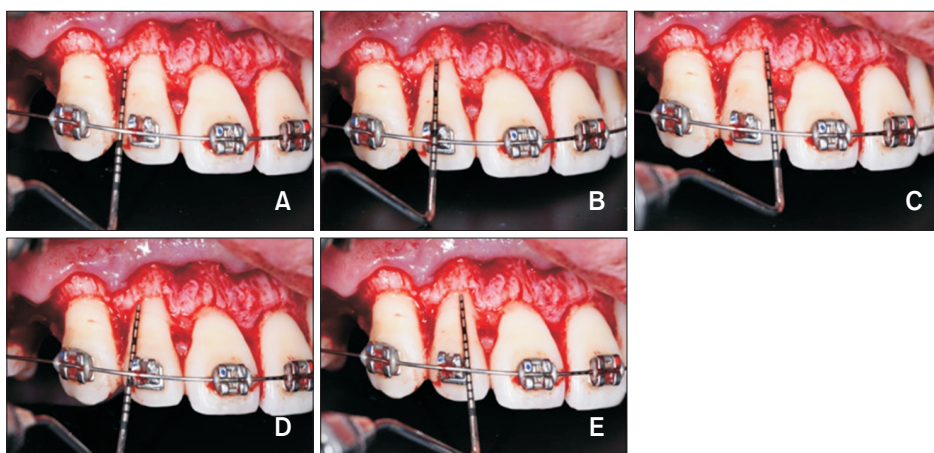


Figure 4. Intraoperative linear measurements. **A–C**, Linear measurements at the distolabial (**A**), midlabial (**B**), and mesiolabial (**C**) sites. **D, E**, Linear measurements at the distobacket (**D**) and mesio-bracket (**E**) sites.

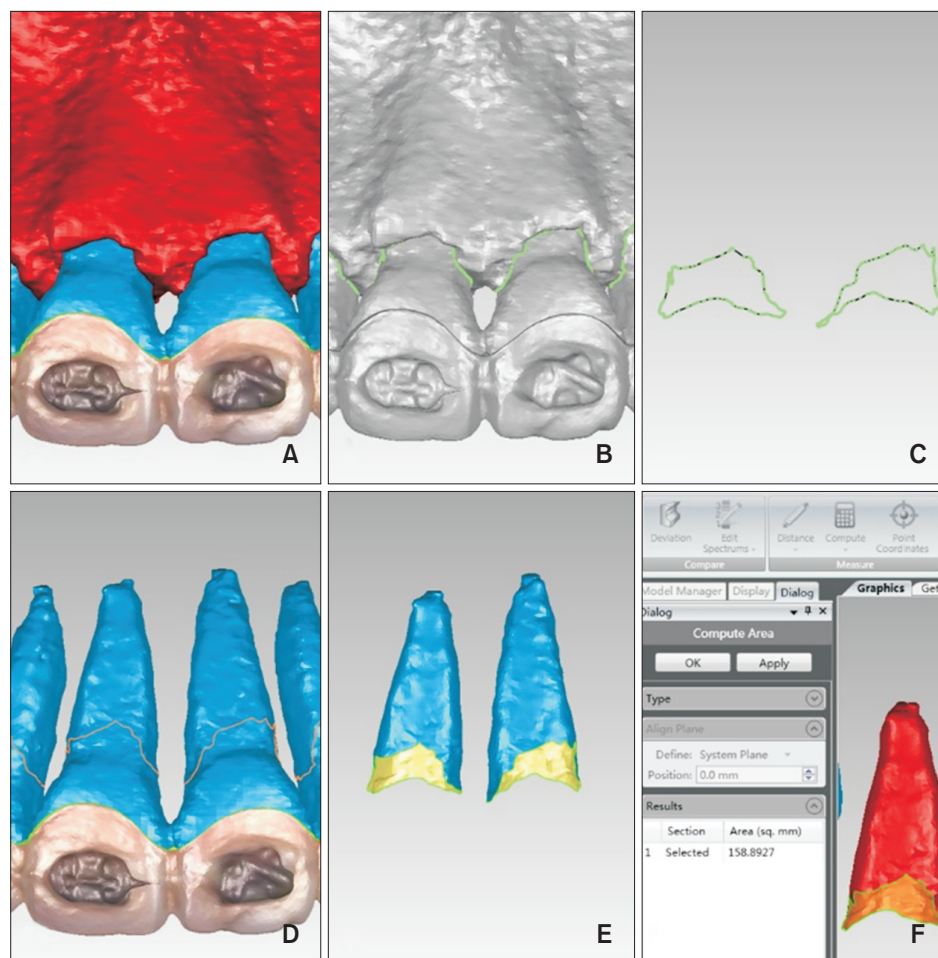


Figure 5. Establishment of digital periodontal ligament (PDL) models. **A**, Tooth and alveolar bone digital models. **B**, The alveolar bone crests are drawn on the tooth models. **C**, The curves of the alveolar bone crests were extracted. **D**, The tooth models are separated along the curves of the alveolar bone crests. **E**, The digital PDL models. **F**, Computation of the PDL area.

assessment relative to the clinical measurement.

$$\text{Measurement difference} = \text{intraoperative measurement} - \text{3D digital measurement}$$

If the measurement difference ranged from -1 to $+1$ mm (including -1 and $+1$ mm), the measurement obtained from the 3D digital image was considered consistent with the intraoperative measurement; otherwise, the measurements were considered inconsistent. Thereafter, the corresponding diagnostic coincidence rates were calculated. To examine the agreement between the digital models obtained by different examiners, 24 randomly chosen teeth were assessed in a blinded manner by two authors with 4–8 years of experience in dental and periodontal imaging. The error was evaluated by measuring the surface area of the PDL in the models. The systematic interexaminer agreement was calculated using the ICC, and the Bland–Altman method was applied to identify the limits of agreement.

RESULTS

Validation of 3D digital model accuracy and consistency according to voxel size

For both the maxillary and mandibular anterior teeth, there were no significant differences in digital measurements at different sites among different voxel sizes ($p > 0.05$ for both); moreover, there were no significant differences between the digital and intraoperative BBD measurements ($p > 0.05$ for both; Table 1).

The maxillary anterior teeth showed no significant differences between the digital and intraoperative VBL measurements ($p > 0.05$; Table 1). However, for the mandibular anterior teeth, except for VBL_La, the digital VBL measurements were smaller than the intraoperative VBL measurements ($p < 0.01$; Table 1).

A statistically significant ICC was found for the correlation between all digital and intraoperative measurements ($p < 0.01$; Table 2), with ICC values ranging from 0.646 to 0.793 for the VBL and from 0.839 to 0.908 for the BBD.

Table 1. Comparison of intraoperative measurements and digital linear measurements at different sites with different voxel sizes

Measurements	Digital			Intraoperative	p-value	Multiple comparison
	0.2 mm	0.25 mm	0.3 mm			
Maxillary anterior teeth						
VBL_MLa (mm)	1.08 ± 0.50	1.06 ± 0.44	1.01 ± 0.47	1.00 ± 0.74	0.22	-
VBL_MB (mm)	1.58 ± 0.53	1.49 ± 0.72	1.39 ± 0.54	1.46 ± 0.66	0.74	-
VBL_La (mm)	1.98 ± 0.57	2.04 ± 0.74	1.93 ± 0.69	1.79 ± 0.72	0.63	-
VBL_DB (mm)	1.68 ± 0.47	1.52 ± 0.59	1.51 ± 0.54	1.60 ± 0.63	0.71	-
VBL_DLa (mm)	1.41 ± 0.63	1.16 ± 0.75	1.01 ± 0.55	1.35 ± 0.76	0.15	-
BBD_MB (mm)	7.47 ± 1.08	7.27 ± 1.07	7.32 ± 0.99	7.33 ± 1.11	0.92	-
BBD_La (mm)	8.09 ± 0.91	7.86 ± 1.03	7.81 ± 1.04	7.96 ± 1.21	0.81	-
BBD_DB (mm)	7.77 ± 0.97	7.32 ± 0.95	7.36 ± 0.98	7.63 ± 0.94	0.32	-
Mandibular anterior teeth						
VBL_MLa (mm)	1.56 ± 0.60	1.30 ± 0.45	1.55 ± 0.57	2.13 ± 0.76	0.000**	Intra > (0.2 mm, 0.25 mm, 0.3 mm)
VBL_MB (mm)	2.54 ± 0.86	2.37 ± 0.79	2.48 ± 0.84	3.31 ± 0.70	0.000**	Intra > (0.2 mm, 0.25 mm, 0.3 mm)
VBL_La (mm)	3.87 ± 1.72	3.69 ± 1.40	3.65 ± 1.56	4.52 ± 1.05	0.15	-
VBL_DB (mm)	2.75 ± 0.86	2.47 ± 1.16	2.39 ± 0.62	3.44 ± 0.97	0.000**	Intra > (0.2 mm, 0.25 mm, 0.3 mm)
VBL_DLa (mm)	1.50 ± 0.58	1.27 ± 0.46	1.51 ± 0.54	2.25 ± 0.81	0.000**	Intra > (0.2 mm, 0.25 mm, 0.3 mm)
BBD_MB (mm)	8.16 ± 1.56	8.01 ± 1.54	7.94 ± 1.50	7.92 ± 1.59	0.95	-
BBD_La (mm)	9.36 ± 2.23	9.42 ± 2.00	9.24 ± 2.20	9.35 ± 1.60	0.99	-
BBD_DB (mm)	8.09 ± 1.52	8.01 ± 1.84	7.78 ± 1.40	7.98 ± 1.77	0.92	-

Values are presented as mean ± standard deviation.

One-way ANOVA with Duncan’s multiple comparison test was performed for comparisons between intraoperative and digital linear measurements.

VBL, vertical bone level; BBD, bone–bracket distance; MLa, mesiolabial; MB, mesiobacket; La, midlabial; DB, distobacket; DLa, distolabial.

**p ≤ 0.01.

Table 2. Intraclass correlation coefficient (ICC) analysis of intraoperative and digital linear measurements obtained with different voxel sizes

Measurements		0.2 mm			0.25 mm			0.3 mm		
		ICC	95% CI		ICC	95% CI		ICC	95% CI	
			Lower bound	Upper bound		Lower bound	Upper bound		Lower bound	Upper bound
Maxillary anterior teeth	VBL	0.793**	0.715	0.851	0.684**	0.576	0.769	0.646**	0.528	0.739
	BBD	0.887**	0.825	0.928	0.850**	0.771	0.904	0.908**	0.857	0.942
Mandibular anterior teeth	VBL	0.726**	0.629	0.801	0.769**	0.684	0.833	0.689**	0.582	0.772
	BBD	0.839**	0.754	0.896	0.872**	0.803	0.918	0.842**	0.758	0.898

VBL, vertical bone level; BBD, bone–bracket distance; CI, confidence interval.

**p ≤ 0.01.

Agreement and reliability of 3D virtual model measurements

The mean differences and descriptive statistics for the measurements are shown in Tables 3 and 4. The mean differences (and 95% CIs) between the digital and intra-

operative measurements for the maxillary anterior teeth were approximately 0; this confirmed no significant differences. Statistically significant mean differences were found in the VBL measurements for the mandibular anterior teeth, regardless of the voxel size (p < 0.01),

Table 3. Descriptive statistics, diagnostic coincidence rates, limits of agreement, and 95% CIs for differences in linear measurements obtained with different voxel sizes for the maxillary anterior teeth

Measurement difference	Mean difference (mm)	Median (mm)	SD (mm)	Range (mm)	Diagnostic coincidence rates (%)	Limits of agreement (mm)	95% CI (mm)
VBL (n = 120)							
0.2 mm	-0.07	-0.10	0.43	2.28	96.66	-0.92-0.78	-0.15-0.00
0.25 mm	-0.01	-0.01	0.58	2.72	92.50	-1.15-1.12	-0.11-0.09
0.3 mm	0.07	0.09	0.58	2.61	90.00	-1.06-1.21	-0.03-0.17
BBD (n = 72)							
0.2 mm	-0.09	0.01	0.51	2.60	90.27	-1.08-0.91	-0.21-0.03
0.25 mm	0.11	0.11	0.59	3.34	94.44	-1.04-1.26	-0.03-0.25
0.3 mm	0.09	0.02	0.47	2.59	97.22	-0.82-1.00	-0.02-0.19

VBL, vertical bone level; BBD, bone-bracket distance; CI, confidence interval; SD, standard deviation.

Table 4. Descriptive statistics, diagnostic coincidence rates, limits of agreement, and 95% CIs for differences in linear measurements obtained with different voxel sizes for the mandibular anterior teeth

Measurement difference	Mean difference (mm)	Median (mm)	SD (mm)	Range (mm)	Diagnostic coincidence rates (%)	Limits of agreement (mm)	95% CI (mm)
VBL (n = 120)							
0.2 mm	0.68	0.71	0.95	5.82	63.33	-1.17-2.54	0.51-0.85
0.25 mm	0.91	0.88	0.85	5.92	56.66	-0.76-2.58	0.75-1.06
0.3 mm	0.82	0.81	0.95	6.58	56.66	-1.05-2.68	0.64-0.98
BBD (n = 72)							
0.2 mm	-0.04	-0.10	0.98	5.03	66.67	-1.96-1.88	-0.26-0.19
0.25 mm	0.11	0.20	0.89	5.13	77.78	-1.65-1.86	-0.10-0.31
0.3 mm	0.17	0.08	0.98	6.23	70.83	-1.76-2.10	-0.06-0.40

VBL, vertical bone level; BBD, bone-bracket distance; CI, confidence interval; SD, standard deviation.

while the mean differences (and 95% CIs) in the BBD measurements were approximately 0.

The diagnostic coincidence rates for the VBL and BBD values for the maxillary anterior teeth were $\geq 90\%$. For the mandibular anterior teeth, the diagnostic coincidence rates ranged from 56.66% to 63.33% for the VBL and from 66.67% to 77.78% for the BBD (Tables 3 and 4).

For validation of the different measurements, the differences between the digital and intraoperative measurements were plotted against the average, as recommended in Bland-Altman analysis. The limits of agreement were defined as $\pm 1.96 \times$ standard deviation and are shown in Figure 6. The limits of agreement for the maxillary anterior teeth showed discrepancies of approximately 2 mm in the measurements. However, high variability was observed in the mandibular measurements, as indicated by the large 95% limits of agreement range of approximately 3.5 mm.

Intraexaminer agreement of linear measurements and PDL area measurements

High intraexaminer agreement was observed for the linear measurements of the digital model. The results showed no significant systematic intraexaminer error ($p > 0.05$), with high intraexaminer reliability (ICC, 0.985; 95% CI, 0.973-0.991).

Differences in PDL area measurements between examiners were also analyzed, and the results showed high interexaminer agreement (ICC, 0.947; 95% CI, 0.871-0.979). Moreover, the Bland-Altman analysis showed good consistency between the two examiners in the process of PDL segmentation in the model. The mean bias for the PDL area (mm^2) was 2.57, with limits of agreement ranging from -17.89 to 23.03 (Figure 7), indicating good consistency between the two examiners in the process of PDL segmentation.

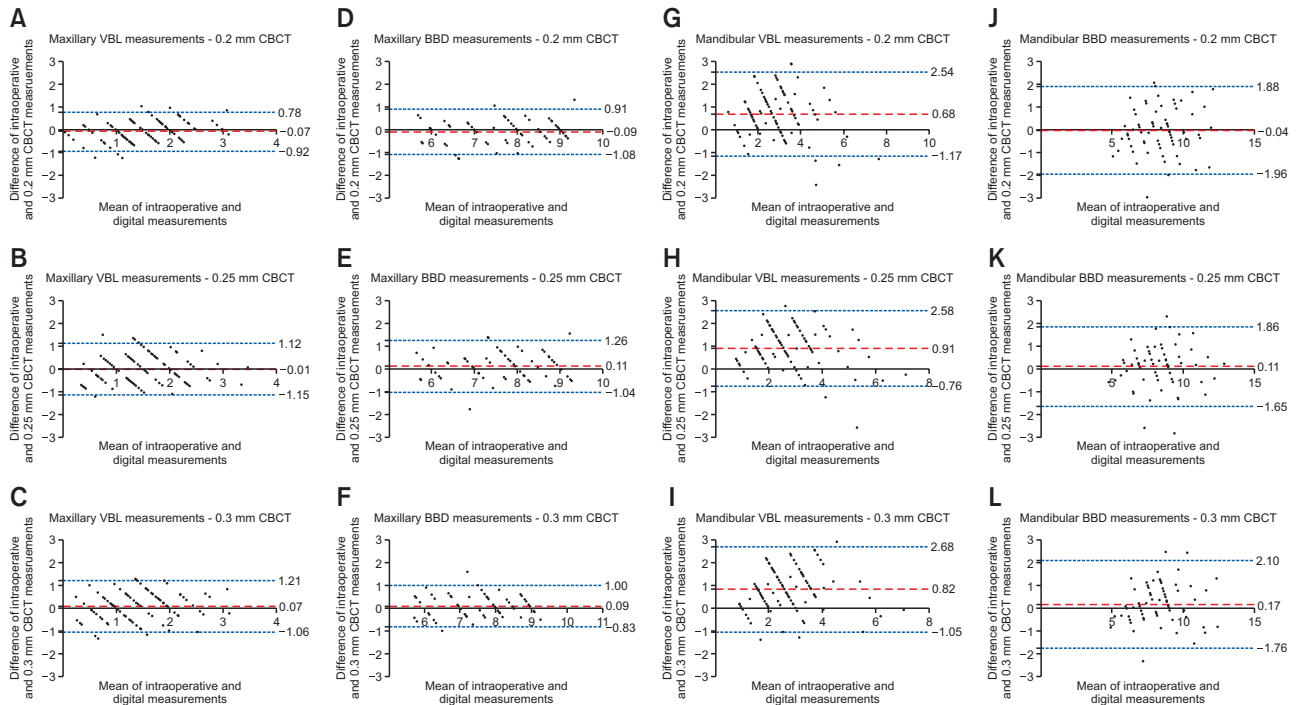


Figure 6. Bland–Altman plots of intraoperative and digital linear measurements with different cone-beam computed tomography (CBCT) voxel sizes. The difference against the mean and the limits of agreement are shown. **A–C**, Vertical bone level (VBL) measurements for the maxillary anterior teeth with different CBCT voxel sizes. **D–F**, Bone–bracket distance (BBD) measurements for the maxillary anterior teeth with different CBCT voxel sizes. **G–I**, VBL measurements for the mandibular anterior teeth with different CBCT voxel sizes. **J–L**, BBD measurements for the mandibular anterior teeth with different CBCT voxel sizes.

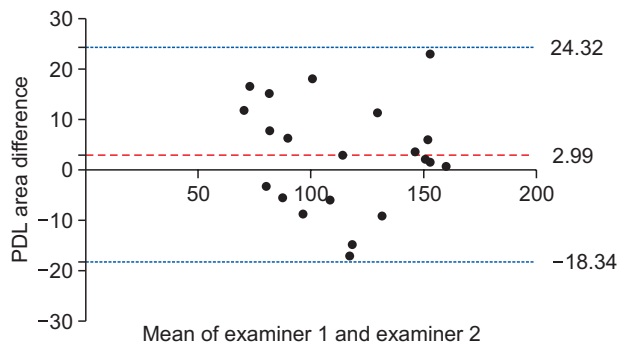


Figure 7. Bland–Altman plots of periodontal ligament (PDL) area measurements by examiner 1 and examiner 2.

Establishment of PDL models

Digital models of the PDL of the maxillary and mandibular anterior teeth of the four patients were successfully established. A representative case is shown in Figure 8.

DISCUSSION

Detection and monitoring of alveolar bone loss are

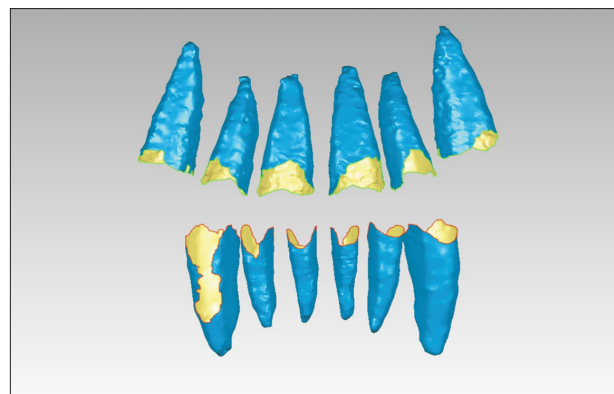


Figure 8. Periodontal ligament models generated for a representative case. The periodontal ligament models of maxillary and mandibular anterior teeth for one of the four patients are shown in Geomagic (Geomagic, Cary, NC, USA).

important because they provide a hard-tissue index for the presence of periodontal disease and the effects of preventative and corrective therapies for periodontal disease.^{22,23} In the present study, we introduced an accurate and reproducible method to obtain alveolar bone crest-

based digital PDL models using 3D CBCT reconstruction.

The present study suggests that 3D CBCT reconstruction provides relatively accurate information regarding the alveolar bone around the anterior teeth. There were no significant differences among measurements obtained using CBCT voxel resolutions of 0.20, 0.25, and 0.30 mm; this indicates that the method is highly valuable for clinical application. Previous studies have shown that discernment of the PDL space requires CBCT data with a resolution capable of detecting structures less than 0.2 mm in size.^{22,24} However, data with higher resolution may require higher levels of radiation, which would increase the radiation exposure of patients.²⁵ The present study shows that CBCT with a voxel size of 0.30 mm and relatively little radiation is sufficient to represent the morphology of the alveolar crest, relative to the gold standard. Furthermore, the position of the alveolar crest can be determined, which helps in identification of the coronal margin of the PDL.

Many previous studies have focused on factors influencing the accuracy of CBCT datasets for 3D reconstruction-based measurements²⁶⁻²⁸ or linear measurements of the alveolar bone, such as the alveolar bone level in the sagittal plane.^{25,29-31} Some studies have shown that a smaller voxel size is associated with better spatial resolution,^{26,27} while others have concluded that there is no significant difference between high-resolution and low-resolution CBCT protocols.^{28,29} A lower resolution also results in higher levels of image noise and influences the accuracy of alveolar bone measurements.^{30,32} This may explain the divergence in conclusions to some extent. Moreover, various exposure parameters in CBCT may influence the image quality, such as the FOV and presence of metallic restorations.^{33,34} In the present study, the FOV, voltage, and other conditions were controlled to investigate the effects of the voxel size. In addition, all patients had metal brackets because CBCT was performed during orthodontic treatment, which is a common clinical situation. Although CBCT can provide an accurate 3D view of the tooth roots and alveolar bone, dense intraoral metal brackets can severely compromise the image quality of crowns.³⁵ Therefore, in this study, intraoral optical scans were used to obtain profiles of anterior tooth crowns and surrounding soft tissue in the STL format, thus eliminating the impact of metal artefacts on the crown morphology.

Previous studies have reported that accurate 3D models of entire dentition could be generated with an intraoral scan superimposed over the CBCT images during orthodontic treatment with brackets.³⁶⁻³⁸ In the present study, the orthodontic brackets were chosen as reference marks for evaluation of the alveolar bone crest. Our results showed that the digital VBL measurements for the mandibular anterior teeth were significantly smaller

than the intraoperative VBL measurements, while there were no significant differences in the BBD at any site between the two methods. This indicates that the main source of deviation in the VBL measurements was selection of the CEJ point. The position of the CEJ around the mandibular anterior teeth on the 3D model tends to be gingivally oriented. Previously, Wang et al.³⁹ found that reconstruction of the crown and root still showed a clear CEJ boundary and a smooth area on the surface. The present study, however, indicated that the CEJ may not be an accurate or reproducible anatomical landmark for mandibular anterior teeth using a 3D model. This finding agrees with Kuralt et al.,⁴⁰ who found that CEJ point selection was the main source of variability in measurements obtained from an intraoral optical scan-derived model. The inaccurate positioning of the CEJ and the difficulty in its identification in the present study may be attributed to the flatter morphology of the mandibular anterior teeth on the labial side and wear of the CEJ.⁴¹ Furthermore, in the reconstruction of mandibular anterior tooth models using CBCT datasets, the maximum inaccuracy was mainly found at the cervical margins.⁴² Therefore, when the CEJ is used as an anatomical landmark for examining the periodontal health status of the mandibular anterior teeth using a 3D model, the possibility of underestimation of the alveolar bone loss severity should be considered.

Because the gold standard in this study was periodontal probe measurements, precision to ± 1 mm with a manual periodontal probe was acceptable. The results showed a high diagnostic coincidence rate ($> 90\%$) for the maxilla and a relatively low for the mandible. The Bland-Altman method showed that the limits of agreement were -1 mm to $+1$ mm for the maxillary anterior teeth; this finding was generally consistent with the results of a previous study.²⁹ However, the broader limits of agreement and the wider span of differences in digital measurements for the mandibular anterior teeth indicate that the mandibular models are less reliable. This could be attributed to the thinner anterior alveolar bone and more vertical bone loss in skeletal Class III patients than in those with Class I patients with normal occlusion,⁷ as well as the difficulty in obtaining accurate measurements of the boundary of thin alveolar bone using CBCT, even with a 0.125-mm-voxel protocol.²⁹

The present study presents a feasible and noninvasive method for obtaining *in vivo* PDL measurements from a digital model. Previous studies^{5,9,10,12,43} have simulated VBL recession *in vitro* and assumed equal alveolar bone height loss at different sites around teeth, which does not truly reflect clinical periodontal conditions. Some researchers have used dry skulls; however, the lack of soft tissue would likely facilitate the detection of bone surfaces, which has been acknowledged as a serious

limitation.³⁰ Researchers have also used intact cadaver heads with soft tissue for their studies; the lack of noise in radiological data, which is normally created by patient movement, probably contributed to the improved results in their studies.^{29,31,44} Although direct clinical measurements and access have a great advantage, the intraoperative measurements routinely used for research purposes in our facility are not optimal in terms of patient safety during surgery and the duration of the examinations, which should be kept as short as possible; these limitations should not be ignored.

Despite the limitations described above, the present study introduced an accurate and consistent method for obtaining PDL measurements from a reconstructed 3D model, which has important implications for clinical treatment. The 3D morphology of the PDL is a significant prognostic indicator in patients with periodontal disease or those undergoing orthodontic therapy, particularly those with previous periodontal bone loss.

CONCLUSIONS

The present study introduced a method for obtaining PDL measurements from 3D reconstructions of *in vivo* CBCT scans. The results showed that CBCT with a voxel size of 0.30 mm reliably provided accurate data regarding the alveolar crest morphology around the maxillary anterior teeth. Thus, measurements obtained with this method may facilitate more thorough and comprehensive evaluations of periodontal conditions.

ACKNOWLEDGEMENTS

None.

AUTHOR CONTRIBUTIONS

Conceptualization: WL. Data curation: HL, XW. Formal analysis: HM. Funding acquisition: XL. Methodology: YW, YZ. Project administration: XL, XW. Visualization: LX, JH. Writing—original draft: HL. Writing—review & editing: XL.

CONFLICTS OF INTEREST

No potential conflict of interest relevant to this article was reported.

FUNDING

This study was supported by the National Program for Multidisciplinary Cooperative Treatment on Major Diseases (PKUSSNMP-201902).

REFERENCES

1. Beertsen W, McCulloch CA, Sodek J. The periodontal ligament: a unique, multifunctional connective tissue. *Periodontol* 2000 1997;13:20-40.
2. de Jong T, Bakker AD, Everts V, Smit TH. The intricate anatomy of the periodontal ligament and its development: lessons for periodontal regeneration. *J Periodontol Res* 2017;52:965-74.
3. Jiang N, Guo W, Chen M, Zheng Y, Zhou J, Kim SG, et al. Periodontal ligament and alveolar bone in health and adaptation: tooth movement. *Front Oral Biol* 2016;18:1-8.
4. Proffit WR, Fields HW, Larson B, Sarver DM. *Contemporary orthodontics*. 6th ed. Philadelphia: Elsevier; 2018.
5. Park SB, An SY, Han WJ, Park JT. Three-dimensional measurement of periodontal surface area for quantifying inflammatory burden. *J Periodontal Implant Sci* 2017;47:154-64.
6. Lee S, Hwang S, Jang W, Choi YJ, Chung CJ, Kim KH. Assessment of lower incisor alveolar bone width using cone-beam computed tomography images in skeletal Class III adults of different vertical patterns. *Korean J Orthod* 2018;48:349-56.
7. Kook YA, Kim G, Kim Y. Comparison of alveolar bone loss around incisors in normal occlusion samples and surgical skeletal class III patients. *Angle Orthod* 2012;82:645-52.
8. Fleiner J, Hannig C, Schulze D, Stricker A, Jacobs R. Digital method for quantification of circumferential periodontal bone level using cone beam CT. *Clin Oral Investig* 2013;17:389-96.
9. Hong HH, Hong A, Huang YF, Liu HL. Incompatible amount of 3-D and 2-D periodontal attachments on micro-CT scanned premolars. *PLoS One* 2018;13:e0193894. Erratum in: *PLoS One* 2018;13:e0209206.
10. Hong HH, Chang CC, Hong A, Liu HL, Wang YL, Chang SH, et al. Decreased amount of supporting alveolar bone at single-rooted premolars is underestimated by 2D examinations. *Sci Rep* 2017;8:45774.
11. Klock KS, Gjerdet NR, Haugejorden O. Periodontal attachment loss assessed by linear and area measurements *in vitro*. *J Clin Periodontol* 1993;20:443-7.
12. Gu Y, Tang Y, Zhu Q, Feng X. Measurement of root surface area of permanent teeth with root variations in a Chinese population—a micro-CT analysis. *Arch Oral Biol* 2016;63:75-81.
13. Al-Rawi B, Hassan B, Vandenberg B, Jacobs R. Accuracy assessment of three-dimensional surface reconstructions of teeth from cone beam computed tomography scans. *J Oral Rehabil* 2010;37:352-8.

14. Wang Y, He S, Guo Y, Wang S, Chen S. Accuracy of volumetric measurement of simulated root resorption lacunas based on cone beam computed tomography. *Orthod Craniofac Res* 2013;16:169-76.
15. Tasanapanont J, Apisariyakul J, Wattanachai T, Sriwilas P, Midtbø M, Jotikasthira D. Comparison of 2 root surface area measurement methods: 3-dimensional laser scanning and cone-beam computed tomography. *Imaging Sci Dent* 2017;47:117-22.
16. Palkovics D, Mangano FG, Nagy K, Windisch P. Digital three-dimensional visualization of intrabony periodontal defects for regenerative surgical treatment planning. *BMC Oral Health* 2020;20:351.
17. Tayman MA, Kamburoğlu K, Küçük Ö, Ateş FSÖ, Günhan M. Comparison of linear and volumetric measurements obtained from periodontal defects by using cone beam-CT and micro-CT: an in vitro study. *Clin Oral Investig* 2019;23:2235-44.
18. Mito T, Sato K, Mitani H. Cervical vertebral bone age in girls. *Am J Orthod Dentofacial Orthop* 2002;122:380-5.
19. Vasir NS, Thompson RT, Davies TM. Dental and skeletal changes following sagittal split osteotomy for correction of mandibular prognathism. *Eur J Orthod* 1991;13:134-42.
20. Forst D, Nijjar S, Flores-Mir C, Carey J, Secanell M, Lagravere M. Comparison of in vivo 3D cone-beam computed tomography tooth volume measurement protocols. *Prog Orthod* 2014;15:69.
21. Jing WD, Jiao J, Xu L, Hou JX, Li XT, Wang XX, et al. Periodontal soft- and hard-tissue changes after augmented corticotomy in Chinese adult patients with skeletal Angle Class III malocclusion: a non-randomized controlled trial. *J Periodontol* 2020; 91:1419-28.
22. Scarfe WC, Azevedo B, Pinheiro LR, Priaminiarti M, Sales MAO. The emerging role of maxillofacial radiology in the diagnosis and management of patients with complex periodontitis. *Periodontol* 2000 2017;74:116-39.
23. Kim DM, Bassir SH. When is cone-beam computed tomography imaging appropriate for diagnostic inquiry in the management of inflammatory periodontitis? An American Academy of Periodontology best evidence review. *J Periodontol* 2017;88:978-98.
24. Choi IGG, Cortes ARG, Arita ES, Georgetti MAP. Comparison of conventional imaging techniques and CBCT for periodontal evaluation: a systematic review. *Imaging Sci Dent* 2018;48:79-86.
25. Spin-Neto R, Gotfredsen E, Wenzel A. Impact of voxel size variation on CBCT-based diagnostic outcome in dentistry: a systematic review. *J Digit Imaging* 2013;26:813-20.
26. Maret D, Telmon N, Peters OA, Lepage B, Treil J, Inglès JM, et al. Effect of voxel size on the accuracy of 3D reconstructions with cone beam CT. *Dentomaxillofac Radiol* 2012;41:649-55.
27. Dong T, Yuan L, Liu L, Qian Y, Xia L, Ye N, et al. Detection of alveolar bone defects with three different voxel sizes of cone-beam computed tomography: an in vitro study. *Sci Rep* 2019;9:8146.
28. Sang YH, Hu HC, Lu SH, Wu YW, Li WR, Tang ZH. Accuracy assessment of three-dimensional surface reconstructions of in vivo teeth from cone-beam computed tomography. *Chin Med J (Engl)* 2016;129:1464-70.
29. Patcas R, Müller L, Ullrich O, Peltomäki T. Accuracy of cone-beam computed tomography at different resolutions assessed on the bony covering of the mandibular anterior teeth. *Am J Orthod Dentofacial Orthop* 2012;141:41-50.
30. Sun Z, Smith T, Kortam S, Kim DG, Tee BC, Fields H. Effect of bone thickness on alveolar bone-height measurements from cone-beam computed tomography images. *Am J Orthod Dentofacial Orthop* 2011;139:e117-27.
31. Wood R, Sun Z, Chaudhry J, Tee BC, Kim DG, Leblebicioglu B, et al. Factors affecting the accuracy of buccal alveolar bone height measurements from cone-beam computed tomography images. *Am J Orthod Dentofacial Orthop* 2013;143:353-63.
32. de-Azevedo-Vaz SL, Vasconcelos Kde F, Neves FS, Melo SL, Campos PS, Haiter-Neto F. Detection of periimplant fenestration and dehiscence with the use of two scan modes and the smallest voxel sizes of a cone-beam computed tomography device. *Oral Surg Oral Med Oral Pathol Oral Radiol* 2013;115:121-7.
33. Icen M, Orhan K, Şeker Ç, Geduk G, Cakmak Özlü F, Cengiz Mİ. Comparison of CBCT with different voxel sizes and intraoral scanner for detection of periodontal defects: an in vitro study. *Dentomaxillofac Radiol* 2020;49:20190197.
34. Pauwels R, Faruangaeng T, Charoenkarn T, Ngonphloy N, Panmekiate S. Effect of exposure parameters and voxel size on bone structure analysis in CBCT. *Dentomaxillofac Radiol* 2015;44:20150078.
35. Harris BT, Montero D, Grant GT, Morton D, Llop DR, Lin WS. Creation of a 3-dimensional virtual dental patient for computer-guided surgery and CAD-CAM interim complete removable and fixed dental prostheses: a clinical report. *J Prosthet Dent* 2017;117:197-204.
36. Lim SW, Moon RJ, Kim MS, Oh MH, Lee KM, Hwang HS, et al. Construction reproducibility of a composite tooth model composed of an intraoral-scanned crown and a cone-beam computed tomography-scanned root. *Korean J Orthod* 2020;50:229-37.
37. Lee RJ, Weissheimer A, Pham J, Go L, de Mene-

- zes LM, Redmond WR, et al. Three-dimensional monitoring of root movement during orthodontic treatment. *Am J Orthod Dentofacial Orthop* 2015;147:132-42.
38. Lee RJ, Pham J, Choy M, Weissheimer A, Dougherty HL Jr, Sameshima GT, et al. Monitoring of tyodont root movement via crown superimposition of single cone-beam computed tomography and consecutive intraoral scans. *Am J Orthod Dentofacial Orthop* 2014;145:399-409.
39. Wang T, Pei X, Luo F, Jia L, Qin H, Cheng X, et al. Evaluation of tooth root surface area using a three-dimensional scanning technique and cone beam computed tomographic reconstruction in vitro. *Arch Oral Biol* 2017;84:13-8.
40. Kuralt M, Gašperšič R, Fidler A. The precision of gingival recession measurements is increased by an automated curvature analysis method. *BMC Oral Health* 2021;21:505.
41. Pini-Prato G, Franceschi D, Cairo F, Nieri M, Rotundo R. Classification of dental surface defects in areas of gingival recession. *J Periodontol* 2010;81:885-90.
42. Maret D, Peters OA, Galibourg A, Dumoncel J, Esclassan R, Kahn JL, et al. Comparison of the accuracy of 3-dimensional cone-beam computed tomography and micro-computed tomography reconstructions by using different voxel sizes. *J Endod* 2014;40:1321-6.
43. Gu Y, Zhu Q, Tang Y, Zhang Y, Feng X. Measurement of root surface area of permanent teeth in a Chinese population. *Arch Oral Biol* 2017;81:26-30.
44. Damstra J, Fourie Z, Huddleston Slater JJ, Ren Y. Accuracy of linear measurements from cone-beam computed tomography-derived surface models of different voxel sizes. *Am J Orthod Dentofacial Orthop* 2010;137:16.e1-6; discussion 16-7.